A Novel Distributed Inter-cell Interference Coordination Scheme based on Projected Subgradient and Network Flow Optimization

Akram Bin Sediq*, Rainer Schoenen*, Halim Yanikomeroglu*, Gamini Senarath§, and Zhijun Chao§
* Department of Systems and Computer Engineering, Carleton University, Ottawa, Ontario, Canada
§ Huawei Technologies Canada CO., LTD.
e-mail: {akram, rs, halim}@sce.carleton.ca, {GaminiS, chaozhijun}@huawei.com

Abstract—In this paper, we propose a novel distributed inter-cell interference coordination (ICIC) scheme. The proposed scheme, which runs in polynomial time, finds a near-optimum dynamic resource partitioning that maximizes a proportional-fairness criterion in the entire network. The proposed scheme is based on primal-decomposition method, where the problem is divided into a master and multiple sub-problems. The master-problem is solved using projected-subgradient method while each of the sub-problems is solved using minimum-cost network flow optimization. Through extensive simulations of four IMT-advanced scenarios, we quantify the gains achieved using the proposed scheme. We demonstrate that the proposed scheme achieves both high cell-edge throughput, that is comparable to frequency reuse 3, and high aggregate throughput, that is at least as good as the aggregate throughput achieved by frequency reuse 1.

Keywords: Dynamic ICIC, Distributed optimization, Scheduling, Subgradient Optimization,

I. INTRODUCTION

Orthogonal Frequency Division Multiple Access (OFDMA) is widely accepted as the multiple access scheme for next generation wireless standards, such as Long-Term Evolution (LTE), LTE-advanced, and WiMax. Among the advantages offered by OFDMA is its scheduling flexibility, since users can be scheduled in both time and frequency, which can be exploited to gain time, frequency, and multi-user diversity.

In order to achieve extremely high data rates in 4G and beyond-4G networks, aggressive frequency reuse is inevitable due to the scarcity of the radio resources. Reuse 1 (universal reuse), in which all radio resources are reused in every sector, is an example of an aggressive frequency reuse scheme. While reuse 1 can potentially achieve high aggregate system throughput, it jeopardizes the throughput experienced by users close to the cell-edge, due to the excessive interference experienced by these users. Therefore, it is vital for the network to use robust and efficient interference mitigation techniques.

Conventionally, interference is mitigated by static resource partitioning and frequency/sector-planning, where close-by sectors are assigned orthogonal resources (clustering). A common example is reuse 3 (cluster size=3 sectors) [1, Section 2.5], where adjacent sectors are assigned orthogonal channels.

Although such techniques can reduce inter-cell interference and improve cell-edge user throughput, they suffer from two major drawbacks. First of all, the aggregate network throughput is significantly reduced since each sector has only a fraction of the available resources, which is equal to the reciprocal of the reuse factor. Secondly, conventional frequency/sector-planning may not be possible in emerging wireless networks where new multi-tier network elements (such as relays, femto-/pico-base-stations) are expected to be installed in an ad hoc manner, without prior planning.

In order to reduce the effect of the first drawback, fractional frequency reuse (FFR) schemes have been proposed. The key idea in FFR is to assign lower reuse factor for users near the cell-center and higher reuse factor for users at the cell-edge. The motivation behind such a scheme is that cell-edge users are more vulnerable to inter-cell interference than cell-center users. Soft Frequency Reuse (SFR) [2] and Partial Frequency Reuse (PFR) [3] are two variations of FFR. While FFR schemes recover some of the throughput lost due to partitioning, they require frequency/cell planning a priori, which is not desirable in future cellular networks as mentioned earlier. As a result, developing efficient dynamic inter-cell interference coordination (ICIC) schemes is vital to the success of future cellular networks.

One approach to tackle the ICIC problem is to devise adaptive FFR or SFR schemes. In [4], an adaptive FFR scheme is proposed where each base-station (BS) chooses one of four reuse modes. A dynamic FFR scheme is proposed in [5] that outperforms conventional FFR schemes in terms of the total system throughput for small cell-sizes; however, no comparison is given for the performance of cell-edge users. In [6], the authors propose softer frequency reuse, which is a heuristic algorithm based on modifying the proportional fair algorithm and the SFR scheme. In [7], the authors proposed gradient-based distributed schemes that create SFR patterns by adjusting the power of the sub-bands.

Another approach to tackle the ICIC problem is to remove the limitations imposed by the FFR or SFR schemes and view the ICIC problem as a multi-cell scheduling problem. In [8], the authors propose a heuristics-based semi-distributed radio resource control scheme where a Radio network controller is assumed to be connected to all BSs. In [9], a graph-theoretic approach is taken to develop an ICIC scheme. In

[10], a game-theoretic approach is pursued and a decentralized algorithm is developed. Nevertheless, the authors observed a significant gap between the proposed scheme and the globally optimum scheme (which is computationally complex). In [11], a heuristics-based centralized ICIC scheme is proposed.

Despite the progress made in ICIC, it is still difficult to assess how close the performance of the existing schemes when compared to the optimal scheme. In this paper, we develop a novel distributed ICIC scheme for downlink transmissions. The proposed scheme, which runs in polynomial time, finds a near-optimum dynamic resource partitioning that maximizes a proportional-fairness criterion in the entire network. We demonstrate through simulations that the proposed scheme achieves both high cell-edge throughput, that is comparable to reuse 3, and high aggregate throughput, that is at least as good as the aggregate throughput achieved by reuse 1.

II. SYSTEM MODEL

We consider the network model described in IMT-advanced [12]. The network layout is shown in Fig. 1 and it consists of K hexagonal sectors served by $K/3$ BSs. Each BS is equipped with a tri-sector antenna to serve a cell-site that consists of 3-sectors. Each BS can communicate with its 6 neighboring BSs; this is supported in upcoming standards (e.g. using the X2 interface in LTE). We focus on the downlink scenario in this paper.

OFDMA is used as the multiple access scheme. The time and frequency radio resources are grouped into time-frequency resource blocks (RBs). RB is the smallest radio resource block that can be scheduled to a user terminal (UT). Each RB consists of N_s OFDM symbols in the time dimension and N_f sub-carriers in the frequency dimension (in LTE, $N_s = 7$ and $N_f = 12$). The total number of RBs is denoted by N.

The number of UTs per sector is denoted by M. Both the BSs and the UTs are assumed to have single antenna each. Similar to [11], we assume that each UT estimates and reports to its serving BS the channel from its serving sector's antenna and from the first-tier interfering sectors. The SINR observed by UT m in sector k on RB n can be expressed as [11]

$$\Gamma_{m,n}^k = \frac{P_C H_{m,n}^{k,k}}{P_C \sum\limits_{\tilde{k}=1, \tilde{k} \neq k}^{K} \left(1 - I_n^{\tilde{k}}\right) H_{m,n}^{k,\tilde{k}} + P_N}, \quad (1)$$
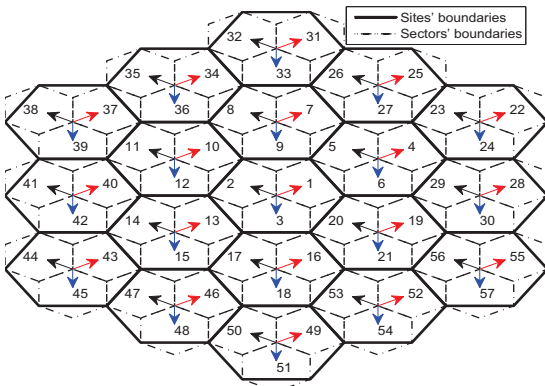

Fig. 1. Network layout consisting of 19 cell sites and 3 sectors per site.

where P_C represents the transmitted power per RB, P_N represents the thermal noise power per RB, $I_n^{\tilde{k}}$ is a binary variable indicating whether RB n is restricted in sector k ($I_n^k = 1$) or not ($I_n^k = 0$), and $H_{m,n}^{k,\tilde{k}}$ represents the channel gain from sector $\tilde{k}$ on RB n to UT m served by sector k. $H_{m,n}^{k,\tilde{k}}$ captures distance-dependant attenuation, shadowing, antenna gains, and multipath fading. The achievable rate on RB n for UT m in sector k is given by

$$R_{m,n}^k = f\left(\Gamma_{m,n}^k\right), \quad (2)$$

where $f(\cdot)$ is the adaptive modulation and coding (AMC) function that maps SINR to rate. Finally, full-buffer traffic model is assumed.

III. PROBLEM STATEMENT

Let us consider a generic scheduler implemented in sector k, without ICIC. This scheduler assigns RB n in subframe t by solving the following optimization

$$\underset{x_{m,n}^k, \forall m}{\text{maximize}} \quad \sum_{m=1}^{M} \alpha_m^k x_{m,n}^k R_{m,n}^k[t] \quad (3a)$$

$$\text{subject to} \quad \sum_{m=1}^{M} x_{m,n}^k = 1, \quad (3b)$$

$$x_{m,n}^k \in \{0,1\}, \quad \forall m, \quad (3c)$$

where α_m^k is the weight for UT m in sector k, $x_{m,n}^k$ are the optimization binary decision variables such that $x_{m,n}^k = 1$ when RB n is assigned to UT m in sector k, and $x_{m,n}^k = 0$ otherwise. Constraint (3b) ensures that each RB is assigned to only one user in sector k. In the case of a proportional fair scheduler (PFS), the weight for UT m is given by $\alpha_m^k = 1/\bar{R}_m^k[t-1]$, where $\bar{R}_m^k[t-1]$ is the average rate for UT m in the previous subframe, averaged over a window of N_{PF} subframes using exponentially-weighted low-pass filter, i.e.,

$$\bar{R}_m^k[t] = \frac{1}{N_{PF}} \sum_{n=1}^{N} x_{m,n}^k R_{m,n}^k[t] + \left(1 - \frac{1}{N_{PF}}\right) \bar{R}_m^k[t-1].$$

To simplify the notation, we drop the subframe index $[t]$ for the rest of the paper. The solution to (3) is given by

$$x_{m,n}^{\star k} = \begin{cases} 1, & m = \arg\max_m \alpha_m^k R_{m,n}^k, \\ 0, & m \neq \arg\max_m \alpha_m^k R_{m,n}^k. \end{cases}$$

We seek to implement an ICIC scheme that maximizes the utility of the network, which is defined as the sum of utilities of all sectors. In doing so, we aim to achieve network-wide proportional fairness[1]. This can be formulated as

$$\underset{x_{m,n}^k, I_n^k, \forall m, k}{\text{maximize}} \quad \sum_{k=1}^{K} \sum_{m=1}^{M} \alpha_m^k x_{m,n}^k R_{m,n}^k \quad (4a)$$

$$\text{subject to} \quad \sum_{m=1}^{M} x_{m,n}^k = 1 - I_n^k, \quad \forall k \quad (4b)$$

$$x_{m,n}^k, I_n^k \in \{0,1\}, \quad \forall m, k, \quad (4c)$$

[1] It is shown in [13] that this strategy achieves proportional fairness as it maximizes $\sum_{m=1}^{M} \log \bar{R}_m^k$ as $N_{PF} \to \infty$.

where the binary variables I_n^k are introduced such that $I_n^k = 1$ when the use of RB n is restricted to sector k and $I_n^k = 0$ otherwise. Constraints (3b) ensure that each RB n is assigned to only one UT in sector k, given that RB n is not restricted in sector k.

The network optimization problem in (4) is difficult to solve for the following reasons. First of all, this problem belongs to the class of non-linear binary combinatorial optimization problems ($R_{m,n}^k$ is a nonlinear function of I_n^k), which are generally difficult to solve in polynomial time. Moreover, the objective function is dependant on the AMC strategy that is used. Hence, an optimal solution for a given AMC strategy may not be optimal for another AMC strategy. Since AMC strategies are operator dependant, it is desirable to develop an algorithm that is independent of the chosen AMC strategy. Finally, it is desirable to solve (4) in a distributed manner since most future standards (such as LTE, LTE-Advanced, WiMax) do not support a central controller. These reasons motivate the proposed algorithm which is explained in the following section.

IV. PROPOSED ALGORITHM

In this section, we show the steps used to develop the proposed algorithm. We start in Section IV-A by introducing a bound and argue that this bound is a good metric for optimization. Using the bound, we get a binary non-linear optimization problem and we transform it into an equivalent binary linear programming (BLP) problem. Next, we relax the resulted BLP problem into a linear programming (LP) problem in Section IV-B. Then, we devise a distributed algorithm using primal-decomposition in Section IV-C. Finally, we present a pseudocode of the proposed algorithm in Section IV-D.

A. Bound Optimization

The SINR expression in (1) can be lower-bounded as

$$\Gamma_{m,n}^k \geq \frac{P_C H_{m,n}^{k,k}}{P_C \sum\limits_{\tilde{k}=1, \tilde{k} \neq k}^{K} H_{m,n}^{k,\tilde{k}} - \max\limits_{\tilde{k} \in \mathcal{K}^k} I_n^{\tilde{k}} P_C H_{m,n}^{k,\tilde{k}} + P_N}, \quad (5)$$

where $\mathcal{K}^k$ is set of indices of the 6 first-tier interfering sectors seen by sector k, e.g., in Fig.1, $\mathcal{K}^3 = \{1, 2, 13, 17, 16, 20\}$ [2]. The bound in (5) is obtained by considering only the most dominant restricted-interferer. This bound is exact if the number of restricted interferes is less or equal to one and it is tight for small number of restricted interferes. This is a good bound to be used for optimization (maximization) for the following reasons. First of all, it can be observed that if the bound is increased by Δ, then the exact expression given by (1) will also increase by at least Δ. Moreover, it is already observed in the literature that most of the gain is obtained by restricting the use of an RB to at most 2 sectors [11]. Finally, and most importantly, based on this bound, we can develop a distributed optimization framework that is applicable to a wide range of schedulers and AMC strategies. This framework can

be implemented very efficiently, and can achieve near-optimal performance, as we will see later.

By substituting (5) in (2), $R_{m,n}^k$ can be bounded as

$$R_{m,n}^k \geq r_{m,n}^k + \max_{\tilde{k}} I_n^{\tilde{k}} \tilde{r}_{m,n}^{k,\tilde{k}}, \quad \text{where} \quad (6)$$

$$r_{m,n}^k = f\left(\gamma_{m,n}^k\right), \tilde{r}_{m,n}^{k\tilde{k}} = \begin{cases} f\left(\tilde{\gamma}_{m,n}^{k,\tilde{k}}\right) - r_{m,n}^k & \tilde{k} \in \mathcal{K}^k, \\ 0 & \tilde{k} \notin \mathcal{K}^k, \end{cases}$$

$$\gamma_{m,n}^k = \frac{P_C H_{m,n}^{k,k}}{P_C \sum\limits_{\tilde{k} \neq k} H_{m,n}^{k,\tilde{k}} + P_N}, \tilde{\gamma}_{m,n}^{k,\tilde{k}} = \frac{P_C H_{m,n}^{k,k}}{P_C \sum\limits_{\tilde{k} \neq k} H_{m,n}^{k,\tilde{k}} - P_C H_{m,n}^{k,\tilde{k}} + P_N}.$$

By substituting (6) in (4), the optimization problem can be expressed as

$$\begin{aligned}
\underset{x_{m,n}^k, I_n^k, \forall m, k}{\text{maximize}} & \quad \sum_{k=1}^{K} \sum_{m=1}^{M} \alpha_m^k x_{m,n}^k \left(r_{m,n}^k + \max_{\tilde{k}} I_n^{\tilde{k}} \tilde{r}_{m,n}^{k,\tilde{k}} \right) \\
\text{subject to} & \quad \sum_{m=1}^{M} x_{m,n}^k = 1 - I_n^k, \quad \forall k \qquad (7a) \\
& \quad x_{m,n}^k, I_n^k \in \{0,1\}, \quad \forall m, k. \qquad (7b)
\end{aligned}$$

The optimization problem (7) is a non-linear binary integer optimization problem, which is in general, difficult to solve. As a result, we convert (7) into the following equivalent BILP problem[3]

$$\begin{aligned}
\underset{\substack{x_{m,n}^k, y_{m,n}^{k,\tilde{k}}, I_n^k \\ \forall m, k, \forall \tilde{k} \in \mathcal{K}^k}}{\text{maximize}} & \quad \sum_{k=1}^{K} \sum_{m=1}^{M} \alpha_m^k \left(x_{m,n}^k r_{m,n}^k + \sum_{\tilde{k}=1}^{K} y_{m,n}^{k,\tilde{k}} \tilde{r}_{m,n}^{k,\tilde{k}} \right) \\
\text{subject to} & \quad \sum_{m=1}^{M} x_{m,n}^k = 1 - I_n^k, \quad \forall k \qquad (8a) \\
& \quad \sum_{\tilde{k} \in \mathcal{K}^k} y_{m,n}^{k,\tilde{k}} \leq x_{m,n}^k, \quad \forall m, k \qquad (8b) \\
& \quad \sum_{m=1}^{M} y_{m,n}^{k,\tilde{k}} \leq I_n^{\tilde{k}}, \quad \forall k, \tilde{k} \qquad (8c) \\
& \quad x_{m,n}^k, y_{m,n}^{k,\tilde{k}}, I_n^k \in \{0,1\}, \quad \forall m, k, \tilde{k}, \qquad (8d)
\end{aligned}$$

where $y_{m,n}^{k,\tilde{k}}$ are introduced as auxiliary variables. While (8) can be solved using branch and bound, it has prohibitive complexity that may grow exponentially in the worst case scenario. As a result, we seek a near-optimal solution to (8) that can be computed efficiently in polynomial time.

B. Linear Programming Relaxation

One can obtain an upper bound on the optimum solution of (8) by relaxing the binary constraints and using real numbers instead of integer or binary valued numbers, and solving the problem as an LP problem. This can be done by replacing (8d) with the following constraint

$$x_{m,n}^k, y_{m,n}^{k,\tilde{k}}, I_n^k \in [0,1], \quad \forall m, k, \tilde{k}. \qquad (9)$$

Let $p_{BLP}^\star$ denote the optimal value of (8), let $p_{LP}^\star$ denote the optimal value of the relaxed version of (8), and let $\hat{p}_{LP}^\star$ denote

---

[2]We assume a wraparound layout so each sector has 6 first-tier interfering sectors. For example, $\mathcal{K}^{25} = \{26, 27, 23, 51, 50, 48\}$

[3]Due to space limitation, the intermediate steps used to transform (7) into (8) are omitted.

the value of the objective function evaluated at the rounded-solution (binary) of the relaxed problem. Then, we have the following inequalities

$$p_{LP}^\star \geq p_{BLP}^\star \geq \hat{p}_{LP}^\star. \tag{10}$$

We define the optimality gap, Δ_{Opt}, in percentage as

$$\Delta_{\text{Opt}} = \frac{p_{BLP}^\star - \hat{p}_{LP}^\star}{p_{BLP}^\star} \times 100\% \leq \frac{p_{LP}^\star - \hat{p}_{LP}^\star}{p_{LP}^\star} \times 100\%, \tag{11}$$

where the inequality follows from (10). As we will show later, by solving the relaxed problem and rounding the solution to the closest binary value, one can obtain a solution that is near-optimal, i.e., with small Δ_{Opt}. However, solving the relaxed problem would require a central controller to be connected to all the BSs, which would have to solve a large LP (which is not supported in future cellular networks standards). Consequently, we seek a distributed optimization method to solve the relaxed version of problem (8).

C. Primal Decomposition

The relaxed version of problem (8) has a special structure. For any set of fixed $I_k^n, \forall k$, the optimization problem can be separated into K optimization problems, each can be solved separately in each sector. In other words, the variables $I_k^n, \forall k$ are coupling (complicating) variables.

Let $\phi^k(I_n^1, \ldots, I_n^K)$ denotes the optimal value of the following optimization problem (for fixed $\{I_n^1, \ldots, I_n^K\}$)

$$\underset{\substack{x_{m,n}^k, y_{m,n}^{k,\tilde{k}} \\ \forall m, \forall \tilde{k} \in \mathcal{K}^k}}{\text{maximize}} \quad \sum_{m=1}^{M} \alpha_m^k \left(x_{m,n}^k r_{m,n}^k + \sum_{\tilde{k}=1}^{K} y_{m,n}^{k,\tilde{k}} \tilde{r}_{m,n}^{k,\tilde{k}} \right) \tag{12a}$$

$$\text{subject to} \quad \sum_{m=1}^{M} x_{m,n}^k = 1 - I_n^k, \tag{12b}$$

$$\sum_{\tilde{k}=1}^{K} y_{m,n}^{k,\tilde{k}} \leq x_{m,n}^k, \quad \forall m \tag{12c}$$

$$\sum_{m=1}^{M} y_{m,n}^{k,\tilde{k}} \leq I_n^{\tilde{k}}, \quad \forall \tilde{k} \tag{12d}$$

$$x_{m,n}^k, y_{m,n}^{k,\tilde{k}}, \in [0,1], \quad \forall m, \forall \tilde{k}. \tag{12e}$$

For reasons that will become apparent, we call (12) subproblem k. Then, the relaxed version of (8) is equivalent to

$$\underset{I_n^k, \forall k}{\text{maximize}} \quad \sum_{k=1}^{K} \phi^k(I_n^1, \ldots, I_n^K) \tag{13a}$$

$$I_n^k \in [0,1], \quad \forall k. \tag{13b}$$

We call (13) the master problem. So, the original problem has been decomposed into a master problem and K subproblems using the primal-decomposition method [14, pp. 3-5].

The master problem can be solved iteratively using the projected subgradient method [15, p. 16]. In each iteration, K subproblems are solved in order to evaluate $\phi^k(I_n^1, \ldots, I_n^K), \forall k$ and a subgradient $[\Lambda_n^{\star 1}, \ldots, \Lambda_n^{\star K}] \in \partial \sum_{k=1}^{K} \phi^k(I_n^1, \ldots, I_n^K)$, where $\partial f(x)$ is the subdifferential of $f(\cdot)$ evaluated at x. $\Lambda_n^{\star k}$ is calculated as $\Lambda_n^{\star k} = -\lambda_n^{\star k} + \sum_{\tilde{k} \in \mathcal{K}^k} \lambda_n^{\star \tilde{k}, k}$, where $\lambda_n^{\star k}$ is

an optimum Lagrange multiplier (dual variable) corresponding to constraint (12b) and $\lambda_n^{\star k, \tilde{k}}, \tilde{k} \in \mathcal{K}^k$ are optimum Lagrange multipliers (dual variables) corresponding to constraints (12d). In order for each sector k to calculate $\Lambda_n^{\star k}$, it requires the knowledge of $\lambda_n^{\star k}$ (which can be obtained locally by solving (12)) and $\lambda_n^{\star \tilde{k}, k}, \tilde{k} \in \mathcal{K}^k$ (which can be exchanged from the neighboring sectors). In other words, each sector k sends $\lambda_n^{k, \tilde{k}}$ for all $\tilde{k}$ sectors that are in the neighborhood of sector k, for all n. The master algorithm then updates its variables according to the following

$$I_n^k := I_n^k + \delta \Lambda_n^k, \forall k, \tag{14}$$

where δ is the step-size which can be chosen using any of the standard methods given in [15, pp. 3-4]. Then, each I_n^k is projected into the feasible set of $[0,1]$ as follows

$$I_n^k := \begin{cases} 0, & I_n^k \leq 0 \\ I_n^k, & 0 < I_n^k < 1 \\ 1, & I_n^k \geq 1. \end{cases} \tag{15}$$

Each sector k exchanges I_n^k with its neighbors and the process is repeated for N_{iter} iterations. Finally, the solution is rounded to the nearest binary value.

The subgradient algorithm is guaranteed to converge to the optimum solution when N_{iter} goes to ∞ [15, p. 6] if δ is chosen properly[4]. In practise, however, the algorithm must terminate after a reasonable number of iterations. A natural question to ask is: how far is the value obtained using finite iterations as compared to the true optimum obtained by solving (8). We investigate this question in Section VI and show that few iterations are sufficient to achieve near-optimality.

Clearly, the proposed algorithm relies heavily on solving the subproblem given by (12). Therefore, it is imperative to solve (12) as efficiently as possible. Interestingly, the subproblem given by (12) has a special structure. If we multiply both sides of constraint (12d) with -1, we get an LP with the following properties. Each variable appears in at most one constraint with a coefficient of $+1$ and at most one constraint with a coefficient of -1. According Theorem 9.9 in [16, p. 315], an LP with such a structure can be transformed into an equivalent *Minimum Cost Network Flow* (MCNF) optimization problem[5].

Converting (12) into an MCNF results in significantly improved computational complexity because MCNF optimization problems are well-studied and very efficient algorithms exist to solve them in strongly polynomial time [16, Chapter 10]. These algorithms perform much faster than a generic LP solver. For example, the enhanced capacity scaling algorithm can solve MCNF with $\mathfrak{n}$ nodes and $\mathfrak{m}$ arcs in $O(\mathfrak{m} \log \mathfrak{n} (\mathfrak{m} + \mathfrak{n} \log \mathfrak{n}))$ [16, p. 395].

D. Pseudocode

A pseudocode of the proposed algorithm is shown in Table I.

It can be shown that the worst-case time complexity of the proposed algorithm implemented in each sector is polynomial[6]

---

[4]In this paper we choose δ to be square summable but not summable, which guarantees convergence as $N_{iter} \to \infty$, by setting $\delta = c/p$, where c is any constant and p is the iteration index.

[5]Due to space limitation, the intermediate steps used to transform (12) into an equivalent MCNF are omitted.

[6]Details of the complexity analysis is omitted due to space limitations.

TABLE I
PROPOSED ICIC ALGORITHM TO BE EXECUTED IN EVERY SECTOR k

- **Initialize** $I_n^k, \forall n, k$.
- **for** $p = 1, \ldots, N_{iter}$
    - **Solve MCNF:** Calculate $x_{m,n}^{\star k}, y_{m,n}^{\star k,\tilde{k}}, \lambda_n^{\star k}$, and $\lambda_n^{\star k,\tilde{k}}, \forall \tilde{k} \in \mathcal{K}^k, \forall n$ by solving (12).
    - **Exchange Subgradients:** Send $\lambda_n^{\star k,\tilde{k}}$ to all sectors $\tilde{k} \in \mathcal{K}^k, \forall n$.
    - **Update:**
        * $\Lambda_n^{\star k} := -\lambda_n^{\star k} + \sum_{\tilde{k} \in \mathcal{K}^k} \lambda_n^{\star \tilde{k},k}$.
        * **Subgradient step:** $I_n^k := I_n^k + \delta \Lambda_n^{\star k}$
        * **Project** I_n^k **into feasible set (15)**.
    - **Exchange** I_n^k: Send I_n^k to all sectors $\tilde{k} \in \mathcal{K}^k, \forall n$.

    end
- **Round the solution:** $I_n^{\star k} := \lfloor I_n^k + 0.5 \rfloor$, $x_{m,n}^{\star k} := \lfloor x_{m,n}^{\star k} + 0.5 \rfloor$

TABLE II
COMMON SIMULATION PARAMETERS USED IN ALL SCENARIOS

Parameter	Assumption or Value
Cellular layout	57 hexagonal sectors (wraparound)
Number of UTs per sector	from 2 to 30
Bandwidth (downlink)	10 MHz
Number of RBs (N)	50
Small-Scale fading model	IMT-advanced channel model [18]
BS antenna gain (boresight)	17 dBi
UT antenna gain	0 dBi
Noise power per RB (P_n)	-114.45 dBm (noise figure=7 dB)
Horizontal and elevation BS ant. pattern	[12, pp. 17-18]

and more precisely, $O\left(NM^2 \left(\log M\right)^2\right)$. Having a polynomial algorithm is crucial for the scalability of the network. Indeed, we observed through extensive simulations that the average simulation time grows as MN, i.e., grows linearly in the number of RBs and the number of UTs.

V. SIMULATION SETUP AND PARAMETERS

We simulated four IMT-Advanced Scenarios, namely, Urban Micro (UMi), Urban Macro (UMa), Rural Macro (RMa), and Suburban Macro (SMa). Table II summarizes the simulation parameters used for all scenarios and Table III shows the scenario-specific parameters. We use the AMC strategy given in [17, pp. 98-99]. Perfect channel estimation is assumed. Each UT is associated with the BS to which it has the highest average received power (excluding shadowing). Details of the system-level simulation procedure are given in [12, Section 7].

VI. SIMULATION RESULTS

In order to develop an efficient algorithm to solve the difficult BILP (8) in a distributed manner, two sources of sub-optimality were introduced, namely, relaxing the integer constraints and solving the master optimization problem in finite iterations. To understand the effect of theses sources of sub-optimality, we present in Table IV the mean and standard deviation of the upper-bound on the optimality gap (11) for different number of iterations. For each number of iterations, we simulated a total of 22,000 instances of the optimization problems for the four IMT-advanced scenarios and different numbers of UTs. In the first subframe, a random initial point is used. In the subsequent subframes, the optimal solution of the previous frame is used as an initial point. It is clear from Table IV that the proposed algorithm converges very quickly to a near-optimum solution. As a result, for the rest of the

TABLE III
IMT-ADVANCED SCENARIO SPECIFICATIONS

Scenario	UMi	UMa	RMa	SMa
Inter-site Distance	200 m	500 m	1732 m	1299 m
BS height	10 m	25 m	35 m	35 m
Min. dist. b/w UT and BS	10 m	25 m	35 m	35 m
Antenna tilt	-12°	-12°	-6°	-6°
Carrier Frequency (GHz)	2.5	2.0	0.8	2.0
Total BS transmit power	41 dBm	46 dBm	46 dBm	46 dBm
Path loss and Shadowing	NLOS [12, p. 31]	NLOS [12, p. 31]	NLOS [12, p. 32]	NLOS [12, p. 32]

simulations, we fixed the number of iterations to be 5, since it produces very small optimality gap.

In Fig. 2, we show the CDF of the normalized time-average UT throughput for four schemes: reuse 1, reuse 3, partial frequency reuse (PFR) [3], and the proposed scheme. Normalization is performed by dividing the user throughput over the total downlink bandwidth, which is 10 MHz. In all schemes, PFS is used. It is clear from the figure that reuse 1 has the worst cell-edge performance[7] (0.066) as compared to the other three schemes, due to the excessive interference experienced at the cell-edge . Reuse 3, PFR, and the proposed scheme achieve normalized cell-edge user throughput of 0.067, 0.077, and 0.077 respectively. However, both reuse 3 and PFR improves the cell-edge performance at the expense of reducing the overall throughput, especially for UTs close to the cell-center. For example, the 95th percentiles (which is an indication of the cell-center UTs) achieved by reuse 3 and PFR are 0.16 and 0.29, respectively, as compared to 0.43 and 0.42 achieved by reuse 1 and the proposed scheme, respectively. Interestingly, the proposed scheme combines the advantages of reuse 1, reuse 3, and PFR, as it provides very good cell-edge throughput and very good center-cell throughput simultaneously. The same trend has been observed from the CDF for UMi, RMa, and SMa scenarios.

In order to take a closer look at the performance of the different schemes, we show in Fig. 3 the normalized cell-edge user throughput and the normalized aggregate sector throughput for all schemes and for different number of UTs, for the UMa scenario. The general trend for all schemes (as expected) is that as M increases, the sector throughput increases due to the increase in multi-user diversity achieved by the channel-aware scheduler (PFS in this case) and the cell-edge user throughput decreases because more UTs share the same resources. For the same number of UTs, we observe that reuse 3, PFR, and the proposed scheme have significantly higher cell-edge throughput than reuse 1, especially for smaller M. On the other hand, it is clear that both reuse 3 and PFR incur significant loss in the aggregate sector throughput. Interestingly, the proposed scheme performs very well in both the cell-edge and the sector throughput as compared to all other schemes.

In Table V, we summarize the gains in aggregate sector throughput and cell-edge user throughput achieved by reuse 3, PFR, and proposed scheme as compared to reuse 1. These gains were obtained for the four IMT-advanced scenarios described in Section V. For each scenario, the number of UTs per sector is varied from 2 to 30. It is clear that the proposed scheme can achieve significant gain in the cell-edge throughput

---

[7]The normalized cell-edge user throughput is defined as the 5th percentile of the normalized user throughput.
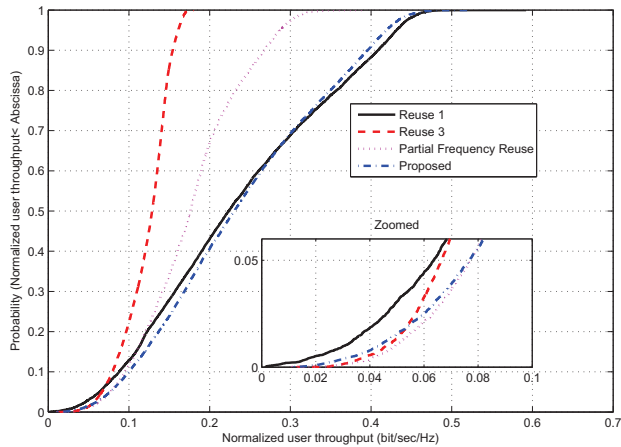
Fig. 2. CDF of the time-average UT throughput of all users in the network for UMa Scenario and 10 users per sector.
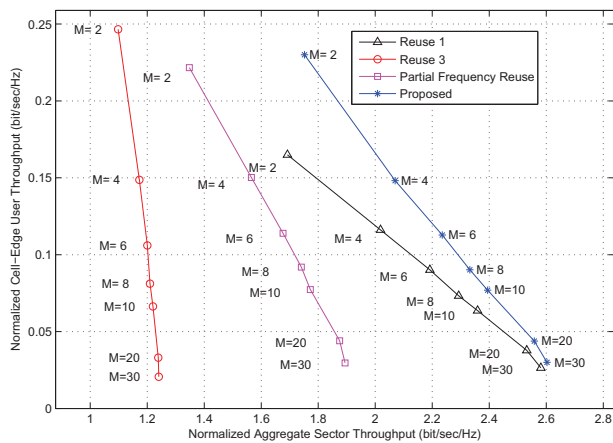

Fig. 3. Normalized cell-edge throughput Vs normalized sector throughput for different schemes in UMa, for different number of users per sector.

(e.g., a gain of 97 % for RMa and M=2) without any penalty on the aggregate sector throughput. Contrarily, both reuse 3 and PFR incur significant loss in the aggregate sector throughput (e.g., a loss of $\approx 40\%$ and $\approx 25\%$, respectively).

VII. CONCLUSIONS

In this paper, we have proposed a novel distributed ICIC scheme that runs in polynomial time and exhibits fast convergence. The proposed scheme is developed using primal-decomposition method, which is used to decompose the problem into a master problem and multiple subproblems. The master problem is solved using projected subgradient method while each of the sub-problems is solved using network flow optimization.

While static partitioning schemes, such as reuse 3 and PFR, can boost the cell-edge user throughput, they incur a penalty on the aggregate network throughput. Through extensive simulation of different IMT-advanced scenarios, we have demonstrated that the proposed algorithm achieves high cell-edge user throughput (comparable to reuse 3 and PFR) without any penalty on the aggregate throughput.

REFERENCES

[1] T. S. Rappaport, *Wireless Communications: Principles and Practice*. Prentice-Hall, 1996.

[2] 3GPP Project Document R1-050 507, "Soft frequency reuse scheme for UTRAN LTE," Tech. Rep., May 2005.

[3] M. Sternad, T. Ottosson, A. Ahlen, and A. Svensson, "Attaining both coverage and high spectral efficiency with adaptive OFDM downlinks," in *Proc. IEEE VTC2003-Fall*, October 2003, pp. 2486–2490.

[4] 3GPP Project Document R1-072 762, "Further discussion on adaptive fractional frequency reuse," Tech. Rep., June 2007.

[5] S. H. Ali and V. C. M. Leung, "Dynamic frequency allocation in fractional frequency reused OFDMA networks," *IEEE Trans. Wireless Commun.*, vol. 8, no. 12, pp. 4286–4295, August 2009.

[6] X. Zhang, C. He, L. Jiang, and J. Xu, "Inter-cell interference coordination based on softer frequency reuse in OFDMA cellular systems," in *Proc. IEEE ICNNSP*, June 2008, pp. 270 –275.

[7] A. Stolyar and H. Viswanathan, "Self-organizing dynamic fractional frequency reuse for best-effort traffic through distributed inter-cell coordination," in *Proc. IEEE INFOCOM 2009*, April 2009.

[8] G. Li and H. Liu, "Downlink radio resource allocation for multi-cell OFDMA system," *IEEE Trans. Wireless Commun.*, vol. 5, no. 12, pp. 3451 –3459, December 2006.

[9] R. Y. Chang, Z. Tao, J. Zhang, , and C. C. J. Kuo, "Multicell OFDMA downlink resource allocation using a graphic framework," *IEEE Trans. Vehicular Technol.*, vol. 58, no. 12, pp. 3494–3507, September 2009.

[10] J. Ellenbeck, C. Hartmann, and L. Berlemann, "Decentralized inter-cell interference coordination by autonomous spectral reuse decisions," in *Proc. The 14th European Wireless Conference, 2008.*, June 2008.

[11] M. Rahman and H. Yanikomeroglu, "Enhancing cell-edge performance: A downlink dynamic interference avoidance scheme with inter-cell coordination," *IEEE Trans. Wireless Commun.*, vol. 9, no. 4, pp. 1414–1425, April 2010.

[12] ITU, Report ITU-R M.2135-1, "Guidelines for evaluation of radio interface technologies for IMT-Advanced," Tech. Rep., December 2009.

[13] P. Viswanath, D. Tse, and R. Laroia, "Opportunistic beamforming using dumb antennas," *IEEE Trans. on Inf. Theory*, vol. 48, no. 6, pp. 1277–1294, June 2002.

[14] S. Boyd, L. Xiao, A. Mutapcic, and J. Mattingley, "Notes on decomposition methods," Lecture notes for EE364B, Stanford University, Feberuary 2007.

[15] S. Boyd and A. Mutapcic, "Subgradient methods," Lecture notes for EE364b, Stanford University, January 2007.

[16] R. Ahuja, T. Magnanti, and J. Orlin, *Network Flows: Theory, Algorithms, and Applications*. Prentice Hall, 1993.

[17] 3GPP TR 36.942 V10.1.0, "Evolved Universal Terrestrial Radio Access (E-UTRA) Radio Frequency (RF) system scenarios (Release 10)," Tech. Rep., October 2010.

[18] CELTIC/CP5-026 Project WINNER+ Document 5D/478-E, "Software implementation of imt.eval channel model," Tech. Rep.

TABLE IV
MEAN AND STANDARD DEVIATION OF THE OPTIMALITY GAP (%)

Number of Iterations	Mean (%)	Standard Deviation (%)
0	43.62	1.16
1	4.61	4.19
2	2.87	3.39
5	1.43	1.43
10	0.95	0.88

TABLE V
GAINS (%) IN SECTOR THROUGHPUT AND CELL-EDGE THROUGHPUT AS COMPARED TO REUSE 1

Scenario	M	Aggregate Sector Throughput			Cell-Edge User Throughput		
		Reuse 3	PFR	Proposed	Reuse 3	PFR	Proposed
UMi	2	-35%	-19%	3%	33%	31%	27%
	6	-45%	-23%	2%	3%	15%	17%
	10	-48%	-25%	1%	-8%	11%	13%
	30	-52%	-27%	1%	-31%	-1%	7%
UMa	2	-35%	-20%	4%	49%	34%	39%
	6	-45%	-24%	2%	18%	26%	25%
	10	-48%	-25%	1%	4%	21%	21%
	30	-52%	-27%	1%	-22%	12%	14%
RMa	2	-35%	-20%	3%	119%	98%	97%
	6	-44%	-23%	1%	55%	54%	41%
	10	-47%	-24%	1%	29%	41%	30%
	30	-50%	-26%	1%	5%	33%	23%
SMa	2	-35%	-22%	3%	138%	106%	93%
	6	-44%	-24%	1%	47%	45%	35%
	10	-47%	-24%	1%	28%	37%	26%
	30	-50%	-26%	1%	2%	31%	21%